Oncogene (2011) 30, 1302–1317

www.nature.com/onc

ORIGINAL ARTICLE

Chromosomal, epigenetic and microRNA-mediated inactivation of LRP1B, a modulator of the extracellular environment of thyroid cancer cells

H Prazeres[1,2,3], J Torres[1], F Rodrigues[4], M Pinto[1], MC Pastoriza[5], D Gomes[6], J Cameselle-Teijeiro[7], A Vidal[5], TC Martins[3], M Sobrinho-Simões[1,2] and P Soares[1,2]

[1]Department of Cancer Biology, Institute of Molecular Pathology and Immunology of the University of Porto (IPATIMUP), Porto, Portugal; [2]Medical Faculty, University of Porto, Porto, Portugal; [3]Department of Molecular Pathology, Service of the Portuguese Institute of Oncology of Coimbra, EPE, Coimbra, Portugal; [4]Department of Endocrinology, Service of the Portuguese Institute of Oncology of Coimbra, EPE, Coimbra, Portugal; [5]Department of Physiology, School of Medicine, University of Santiago de Compostela-Institute of Sanitary Research (IDIS), Santiago de Compostela, Spain; [6]Anatomic Pathology Service of the Portuguese Institute of Oncology of Coimbra, EPE, Coimbra, Portugal and [7]Department of Anatomic Pathology, Clinical University Hospital (CHUS), SERGAS, University of Santiago de Compostela, Santiago de Compostela, Spain

The low-density lipoprotein receptor-related protein (LRP1B), encoding an endocytic LDL-family receptor, is among the 10 most significantly deleted genes across 3312 human cancer specimens. However, currently the apparently crucial role of this lipoprotein receptor in carcinogenesis is not clear. Here we show that LRP1B inactivation (by chromosomal, epigenetic and microRNA (miR)-mediated mechanisms) results in changes to the tumor environment that confer cancer cells an increased growth and invasive capacity. LRP1B displays frequent DNA copy number loss and CpG island methylation, resulting in mRNA underexpression. By using CpG island reporters methylated *in vitro*, we found that DNA methylation disrupts a functional binding site for the histone-acetyltransferase p300 located at intron 1. We identified and validated an miR targeting LRP1B (miR-548a-5p), which is overexpressed in cancer cell lines as a result of 8q22 DNA gains. Restoration of LRP1B impaired *in vitro* and *in vivo* tumor growth, inhibited cell invasion and led to a reduction of matrix metalloproteinase 2 in the extracellular medium. We emphasized the role of an endocytic receptor acting as a tumor suppressor by modulating the extracellular environment composition in a way that constrains the invasive behavior of the cancer cells.
Oncogene (2011) **30,** 1302–1317; doi:10.1038/onc.2010.512; published online 8 November 2010

Keywords: tumor suppressor gene; low-density lipoprotein receptor family; EP300 histone-acetyltransferase; microRNA; matrix metalloproteinase 2; endocytosis and tumor microenvironment

Correspondence: Dr P Soares, Department of Cancer Biology, Institute of Molecular Pathology and Immunology of the University of Porto (IPATIMUP), Rua Dr Roberto Frias s/n, Porto 4200-465, Portugal.
E-mail: psoares@ipatimup.pt
Received 21 June 2010; revised 14 September 2010; accepted 29 September 2010; published online 8 November 2010

Introduction

The low-density lipoprotein receptor-related protein gene (LRP1B) originally isolated on the basis of homozygous deletions detected in human lung cancer cell lines (Liu *et al*., 2000a, 2000b; Kohno *et al*., 2010) was recently reported among the top 10 most significantly deleted genes across 3312 human cancer specimens (Beroukhim *et al*., 2010). LRP1B encodes for a member of the endocytic low-density lipoprotein receptor superfamily. The classical role of LRPs is to mediate the clearance of a myriad of extracellular ligands from the pericellular environment (Herz and Strickland, 2001; May *et al*., 2007). Among these ligands are lipoprotein complexes, trimeric complexes of urokinase plasminogen activator (uPA), plasminogen activator inhibitor type 1 and uPA receptor (Herz *et al*., 1992; Nykjaer *et al*., 1992), as well as matrix metalloproteinases (MMPs) (Emonard *et al*., 2005). LRP1B is most highly expressed in the brain and thyroid gland (Liu *et al*., 2001; Asami *et al*., 2009), and a susceptibility *locus* for familial non-medullary thyroid cancer (fNMTC) at 2q21 (McKay *et al*., 2001), encompassing LRP1B, as well as loss of heterozygosity at 2q21 has been detected in familial (Prazeres *et al*., 2008) and sporadic non-medullary thyroid cancer (NMTC) (Stankov *et al*., 2004). For these reasons, we undertook the present study to elucidate the mechanisms of LRP1B inactivation in cancer cells and to investigate the key roles of this lipoprotein receptor in the carcinogenesis of familial and sporadic thyroid tumors.

Results

Global gene expression profile of familial and sporadic NMTC tumors filters LRP1B as the only significant deregulated gene at 2q21

LRP1B first came to our attention in the study of the individual tumors of an fNMTC family member with a presumable 2q21 susceptibility haplotype

(Supplementary Figure S1A). We performed gene expression profiling in the only tumor (out of four) without loss of heterozygosity at 2q21 by using Affymetrix U133A Plus 2.0 Genechips (Affymetrix, Santa Clara, CA, USA). Among the probesets which encompass the 2q21 region (>200 probesets; 64 candidate genes, Supplementary Table S1), LRP1B was the only gene found to be deregulated. In complement, analysis of 2q21 probesets was done in the data set derived from expression profiling (Affymetrix Human Exon 1.0 ST Array, Affymetrix) of a validation series comprising sporadic thyroid tumors (12 normal samples, 12 follicular thyroid adenomas (FTA) and 18 follicular thyroid carcinomas). Concordantly, we found that LRP1B was the single probeset in 2q21 region showing significant deregulation (threefold cutoff) in sporadic tumors (Supplementary Table S2). Quantitative real-time–PCR (qRT–PCR) was used to validate the results obtained with the microarrays. LRP1B was shown to be downregulated to similar levels in the two fNMTC samples when assessed by complementary (c)DNA microarray or qRT–PCR (−12.15 and −10.1, respectively, Figure 1a). Furthermore, LRP1B was completely silenced or downregulated to variable levels in all the thyroid cancer cell lines analyzed (Figure 1a), suggesting that LRP1B might be relevant in the carcinogenesis of both familial and also sporadic thyroid cancer. We sequenced, in the index family member, the 16 kbp of the entire coding sequence (91 exons) and flanking intron boundaries of LRP1B, as well as cDNA fragments encompassing several exons.

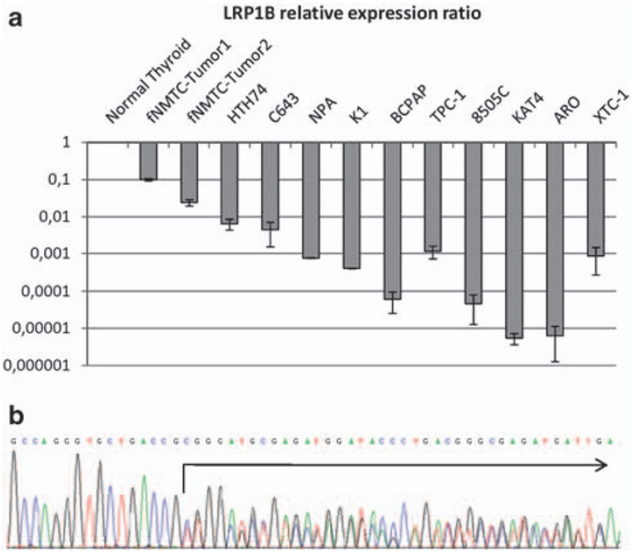

Figure 1 LRP1B is silenced in fNMTC tumors and in thyroid cancer cell lines and is subjected to genetic mutation in a sporadic NMTC. (**a**) mRNA expression of LRP1B in thyroid cancer cell lines, normal thyroid and tumors derived from the index fNMTC case (fNMTC-tumor1 and fNMTC-tumor2). Expression values were normalized to the endogenous control and divided by the relative expression of the normal thyroid sample. (**b**) Sequencing chromatogram, illustrating a LRP1B deletion mutation encompassing exon 1 to exon 2 (del68_146 at the transcript level) detected in one out of five sporadic NMTCs scanned for LRP1B mutations. The arrow indicates the deletion site after which an overlap of the wild-type and deleted alleles is observed.

Aside from previously reported single-nucleotide polymorphisms and intronic variants of unknown significance (Supplementary Figure S1B), we were unable to detect any causative germline mutation in the fNMTC case studied. We additionally screened for mutations in five sporadic thyroid tumor DNAs. In one sporadic non-medullary thyroid cancer, we could demonstrate a frameshift deletion: del68_146 at the transcript level (nucleotide +1 is the ATG initiation codon), which is predicted to translate a truncated LRP1B protein (Figure 1b).

Genomic loss of LRP1B is frequent in sporadic thyroid tumors

As LRP1B was initially identified by the observation of homozygous deletion in lung cancer cell lines, which led to the initial designation of *LRP-DIT*—a gene found to be deleted in tumors, we were prompted to investigate whether LRP1B is subjected to genomic loss. For this purpose, we used genomic qRT–PCR assays directed at LRP1B sequences in the upstream, middle and downstream parts of the gene (exons 5, 44 and 90, respectively), as well as sequences near the chromosome 2 centromere. We found that LRP1B frequently displays genomic loss both in cell lines (5/10, Figure 2a) and also in sporadic tumors (13/20 FTAs, 13/15 follicular thyroid carcinomas (FTCs), 14/19 papillary thyroid carcinomas (PTCs) and 6/10 undifferentiated thyroid carcinomas (UTCs); Figure 2b). In most cases, losses at LRP1B are accompanied by loss at the centromeric locus, indicating that probably the entire chromosomal arm was deleted (Figure 2b). We could observe cases in which copy number values dropped in internal exons of LRP1B, indicating that the deletion breakpoints were intragenic (for example, PTC-14). We could also detect cases with a presumable homozygous loss, displaying a calculated copy number value close to zero (Figure 2b).

LRP1B underexpression follows thyroid cancer progression and correlates with vascular invasion

We analyzed the expression levels of LRP1B at the mRNA level. In accordance with the results observed in thyroid cancer cell lines, we found underexpression at variable degrees, both in pre-malign lesions, such as FTA, as well as in carcinomas, such as FTC, PTC and UTC (Figure 3a). The only case of UTC displaying normal LRP1B mRNA expression was shown to harbor the above-mentioned somatic frameshift mutation (Figure 1B). Noteworthy, the expression level of LRP1B was significantly lower in thyroid lesions, compared with normal thyroid tissue ($P<0.02$), and the expression in UTCs was significantly lower than in differentiated thyroid cancers ($P=0.036$, Figure 3b). The levels of LRP1B were significantly lower in cases with vascular invasion compared with cases without vascular invasion, namely in FTC ($P=0.04$, Figure 3c). A statistically significant underexpression of LRP1B was reproduced in the validation set comprising 12 FTAs and 18 FTCs compared against 12 normal thyroid samples ($P=0.03$, Figure 3d). This was further confirmed in cases in which paired normal and tumor specimens were available

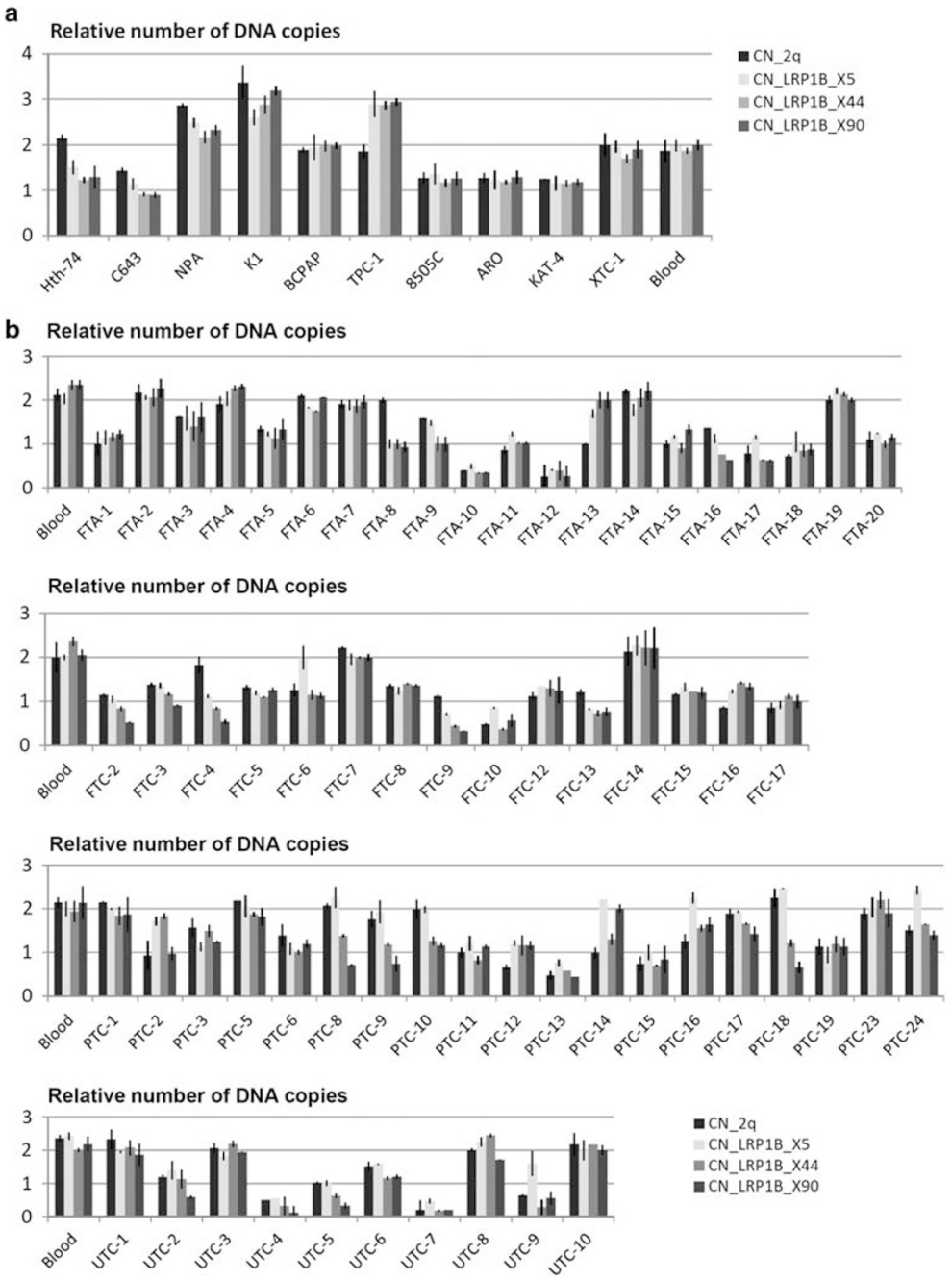

Figure 2 Genomic loss of LRP1B is frequently found in thyroid cancer cell lines and sporadic thyroid tumors. LRP1B DNA copy number in 10 thyroid cancer cell lines (**a**) and thyroid lesions (20 FTAs, 15 FTCs, 19 PTCs and 10 UTCs) (**b**) was determined by genomic quantitative real-time PCR employing primer/probe pairs targeting different genetic regions of LRP1B, namely exon 5, 44 and 90 (CN_LRP1B_X5; _X44 and_X90) and at a region near the 2q centromere (CN_2q). The abundance of DNA copies at each site was normalized to an endogenous control for RNAse P run in multiplex reactions and copy number values were calibrated by performing reactions with blood-derived DNA sample in the same plate. Data were generated with the CopyCaller software.

($P = 0.015$, Figure 3e). However, the association with vascular invasion was not statistically significant in the validation series.

DNA methylation disrupts a transcription factor binding site for p300 at LRP1B intron 1

We asked whether DNA methylation or other epigenetic factors allowed explanation for the observed transcriptional downregulation of LRP1B. By bisulfite sequencing two fragments of the LRP1B CpG island, we detected DNA methylation in 6/10 cell lines and in 10/19 FTAs, 9/16 FTCs, 11/17 PTCs and 5/7 UTCs (Figure 4a). No methylation was observed in any of the normal thyroid samples, confirming that the observed methylation is tumor-specific and excluding the possibility that the observe methylation constitutes tissue-specific methylation (Figure 4a). The pattern

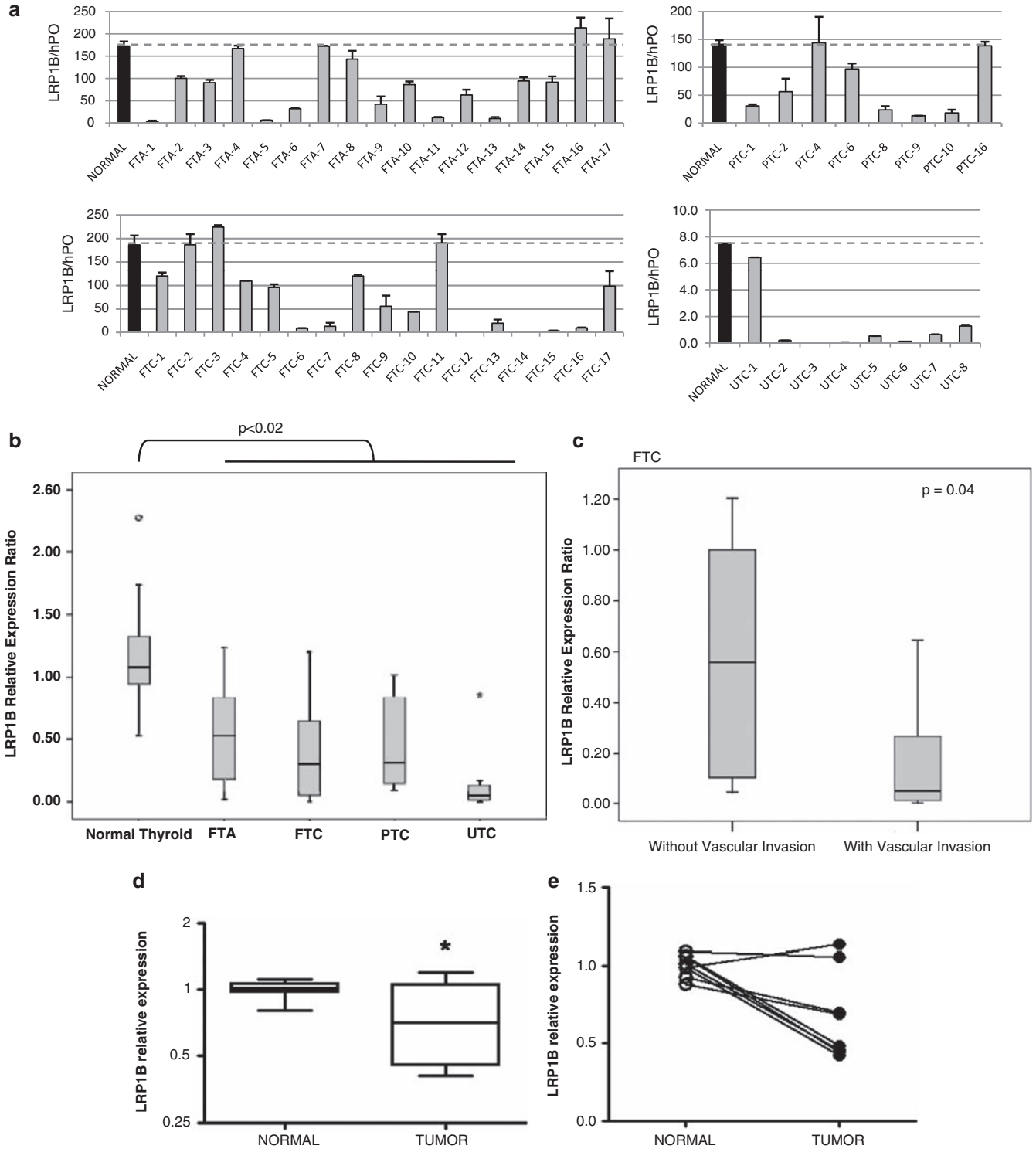

Figure 3 LRP1B underexpression follows thyroid cancer progression and correlates with vascular invasion. (**a**) Real-time PCR quantification of the LRP1B transcript in mRNA samples derived from micro-dissected thyroid lesions. Expression values were normalized to an endogenous control (hPO) and a normal reference (a pool of nine mRNAs obtained from normal thyroid samples subjected to the same treatment as the other cases) was quantified in triplicate in the same plate. (**b**) Differences in the relative expression ratios for each histotype of thyroid lesions are displayed in box-plot graphics. LRP1B is significantly underexpressed in thyroid tumors relative to normal thyroid, and in UTC versus differentiated thyroid tumors (FTC and PTC). In the graphics, open circle (○) or asterisk (*) refer to the outlier cases. Statistical significance *P*-values were obtained by using the Mann–Whitney test. (**c**) LRP1B mRNA levels are significantly lower in FTCs with vascular invasion. (**d**) In a validation series gathered by an independent group and analyzed by a different method (exon arrays), LRP1B is reproducibly found to be underexpressed in tumor versus normal thyroid tissue. (**e**) This observation is further confirmed when paired normal and tumor material was analyzed.

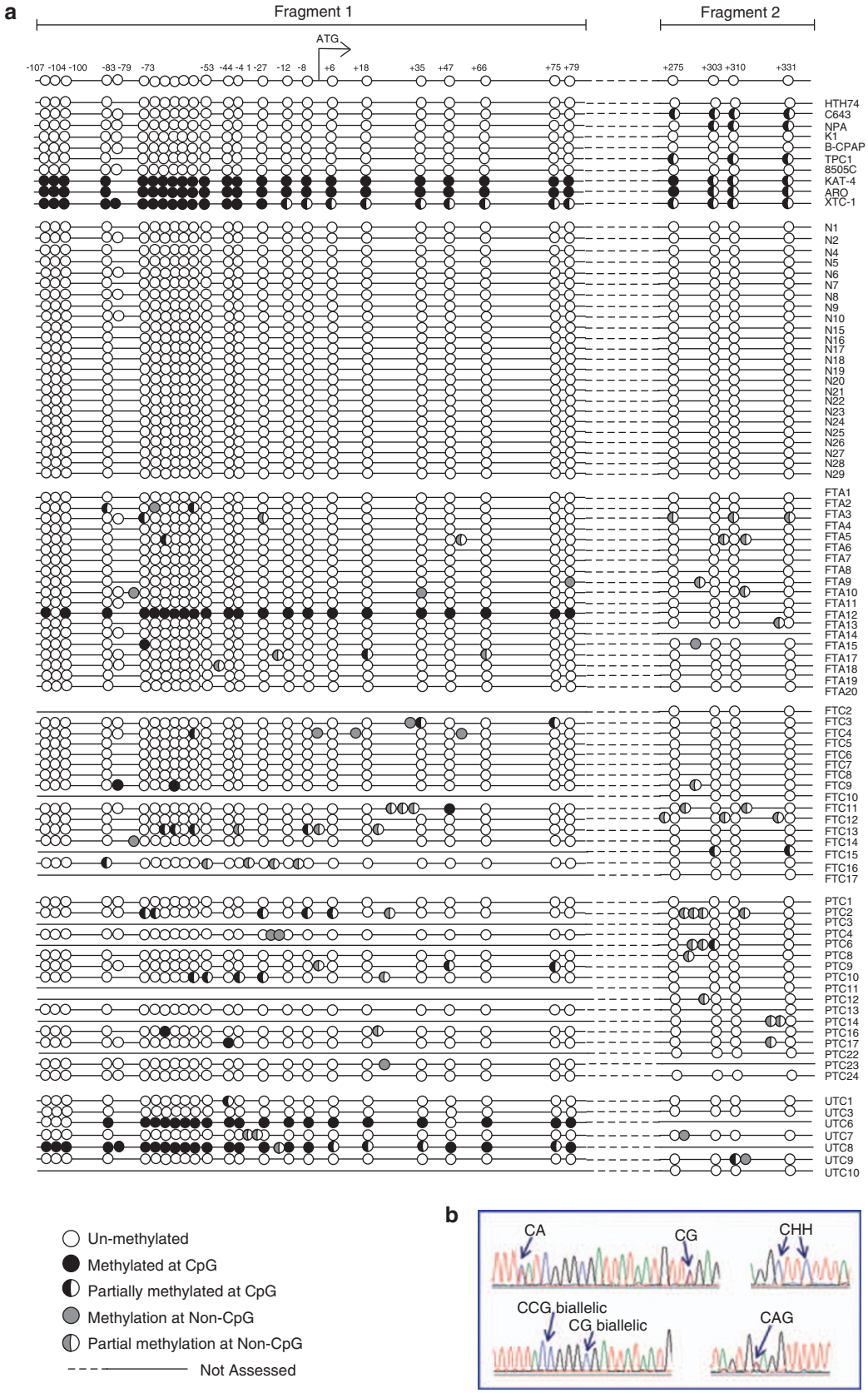
a
Fragment 1
Fragment 2
ATG
-107 -104 -100 -83 -79 -73 -53 -44 -4 1 -27 -12 -8 +6 +18 +35 +47 +66 +75 +79 +275 +303 +310 +331
HTH74
C643
NPA
K1
B-CPAP
TPC1
8505C
KAT-4
ARO
XTC-1
N1
N2
N4
N5
N6
N7
N8
N9
N10
N15
N16
N17
N18
N19
N20
N21
N22
N23
N24
N25
N26
N27
N28
N29
FTA1
FTA2
FTA3
FTA4
FTA5
FTA6
FTA7
FTA8
FTA9
FTA10
FTA11
FTA12
FTA13
FTA14
FTA15
FTA17
FTA18
FTA19
FTA20
FTC2
FTC3
FTC4
FTC5
FTC6
FTC7
FTC8
FTC9
FTC10
FTC11
FTC12
FTC13
FTC14
FTC15
FTC16
FTC17
PTC1
PTC2
PTC3
PTC4
PTC6
PTC8
PTC9
PTC10
PTC11
PTC12
PTC13
PTC14
PTC16
PTC17
PTC22
PTC23
PTC24
UTC1
UTC3
UTC6
UTC7
UTC8
UTC9
UTC10
Un-methylated
Methylated at CpG
Partially methylated at CpG
Methylation at Non-CpG
Partial methylation at Non-CpG
Not Assessed
b
CA
CG
CHH
CCG biallelic
CG biallelic
CAG

of methylation was heterogeneous, without evidence of preferential methylation of a particular CpG (Figure 4a). However, our attention was caught by the observation of methylation in both CpG and non-CpG sites (Figure 4b, inset). The prevailing assumption is that DNA methylation in the mammalian genome is restricted to CpGs. Nonetheless, evidence for a class of non-CpG methylation in mammalian cells comes from several previous studies (Toth *et al*., 1990; Clark *et al*., 1995; Woodcock *et al*., 1997; Malone *et al*., 2001), and recently it was reported in the first complete sequence of the human DNA methylome (Lister *et al*., 2009) that non-CpG sites comprised as much as 25% of methylated cytosines in a human embryonic stem cell line. A fundamental question raised by these results was regarding the functional significance of apparently stochastic methylation in CpG and non-CpG contexts. Analysis of all the sites found to be methylated in non-CpGs in cell lines and tumors indicated that 1/3 of all sites occur in the sequence *CCGG, with methylation of the external C. To address this question, CpG island luciferase reporters with two fragments of the promoter region were generated (fragments A and B). We differentially methylated CpG island luciferase reporters by *in vitro* methylation with bacterial methyltransferases M.Sss-I (*CG), M.Msp-I (*CCGG) and M.Hpa-II (C*CGG) (Figure 5a, chromatograms in Supplementary Figure S2). We found luciferase activity to be increased by the unmethylated fragments of the CpG island (Figure 5a). As expected, complete M.Sss-I-mediated methylation of all *CpGs resulted in abrogation of luciferase activity to values similar to the empty vector. Interestingly, low-density methylation induced by M.Msp-I and M.Hpa-II impaired the transcriptional activity of the reporter-containing fragment B of the CpG island, but not the fragment A reporter (Figure 5a). We reasoned that DNA methylation might interfere with the binding of putative transcription factors to the specific sequences flanking CCGG in fragment B. Using TFSEARCH 1.3 (Heinemeyer *et al*., 1998), we found that a binding motif for the p300 histone-acetyltransferase (GGGAGTG) (Rikitake and Moran, 1992) was present immediately upstream of one of the M.Msp-I/M.Hpa-II CCGG sites (CCGGGAGTG). These observations led us to investigate whether p300 activates the expression of LRP1B and if this effect is methylation sensitive. For this purpose, we transfected HEK293 cells with unmethylated or methylated luciferase constructs of fragment B, either with or without the addition of a p300 expression vector. We found that addition of p300 increased the luciferase activity of the unmethylated construct. However, the p300 enhancer effect was abrogated when either M.Msp-I or M.Hpa-II methylated versions of the reporter were used (Figure 5b). In order to confirm the direct binding of p300 to this LRP1B sequence and its possible perturbation by DNA methylation, we performed proximity ligation assay (Gustafsdottir *et al*., 2007) using DNA probes in the unmethylated, methylated and mutated forms. We showed a 64-fold increase in interactions between p300 and a DNA probe composed of the LRP1B intron 1 unmethylated sequence as compared with probes with a mutated binding site or with methylated *CG and *CCG sites (Figure 5c). In complement to this, we transfected HEK293 and C643 cells with a small interfering RNA designed to inhibit the endogenous p300 and could demonstrate a concomitant reduction in LRP1B expression (Figure 5d). Overall, these results indicate that there is a functional p300 binding site at intron 1 of LRP1B, which could be disrupted by DNA methylation of the flanking CCG sequence. Moreover, these findings highlight the possibility that methylation at unique cytosines, even in a stochastic or non-CpG context, may affect gene transcription, by interfering with *cis* regulatory elements.

Finally, because our findings highlight a role for DNA methylation and histone acetylation in regulation of LRP1B expression, we decided to check whether the use of a DNA-demethylating agent, 5-Aza-2′-deoxycytidine (5AZA), or a histone deacetylase inhibitor, Trichostatin A (TSA), could restore the expression of *LRP1B* mRNA *in vitro*. In cell lines ARO and XTC-1, in which we previously demonstrated LRP1B promoter DNA methylation (Figure 4a), we could show that LRP1B is re-expressed by use of 5AZA or TSA either alone (ARO) or in combination (XTC-1) (Figure 5e).

Overexpression of miR-548a-5p caused by genomic gain at 8q22.3 leads to LRP1B downregulation

Despite the generalized silencing of LRP1B, only three cell lines displayed widespread DNA methylation, and although p300 levels were downregulated in cell lines, they do not appear to account for the differences in the degree of LRP1B downregulation (Supplementary Figure S3). MicroRNAs (miRs) have emerged as alternative mediators of tumor suppressor gene inactivation (Nagel *et al*., 2008) by means of inhibition of translation and/or reducing mRNA stability. We investigated whether overexpression of putative miRs that target LRP1B could be an additional mechanism of LRP1B inactivation. To this end, we started by computationally nominating potential miRs that may target the LRP1B 3′UTR and 5′UTR using the MirBase, TargetScan and MicroInspector prediction

Figure 4 DNA methylation at the LRP1B CpG island disrupts a transcription factor binding site for p300 at intron 1. (**a**) Profile of DNA methylation of the LRP1B CpG island in thyroid cancer cell lines, normal thyroid samples and thyroid tumors. Methylation analysis was performed by bisulfite-PCR-sequencing of two independent fragments of the CpG island (fragment 1: −131 to +100 and fragment 2: +217 to +365, counting from ATG) in 10 thyroid cancer cell lines and in 19 FTAs, 16 FTCs, 17 PTCs and 7 UTCs. Methylation status was also assessed in 24 samples of normal thyroid tissue. Circles represent CpG and non-CpG sites in different configurations: ○—un-methylated; ●—fully methylated; ◐—partially methylated; ◉—fully methylated in a non-CpG site and ◐—partial methylation at a non-CpG. (**b**) This inset contains bisulfite-sequencing chromatograms illustrating sites of non-CpG methylation; H stands for C; A or T.

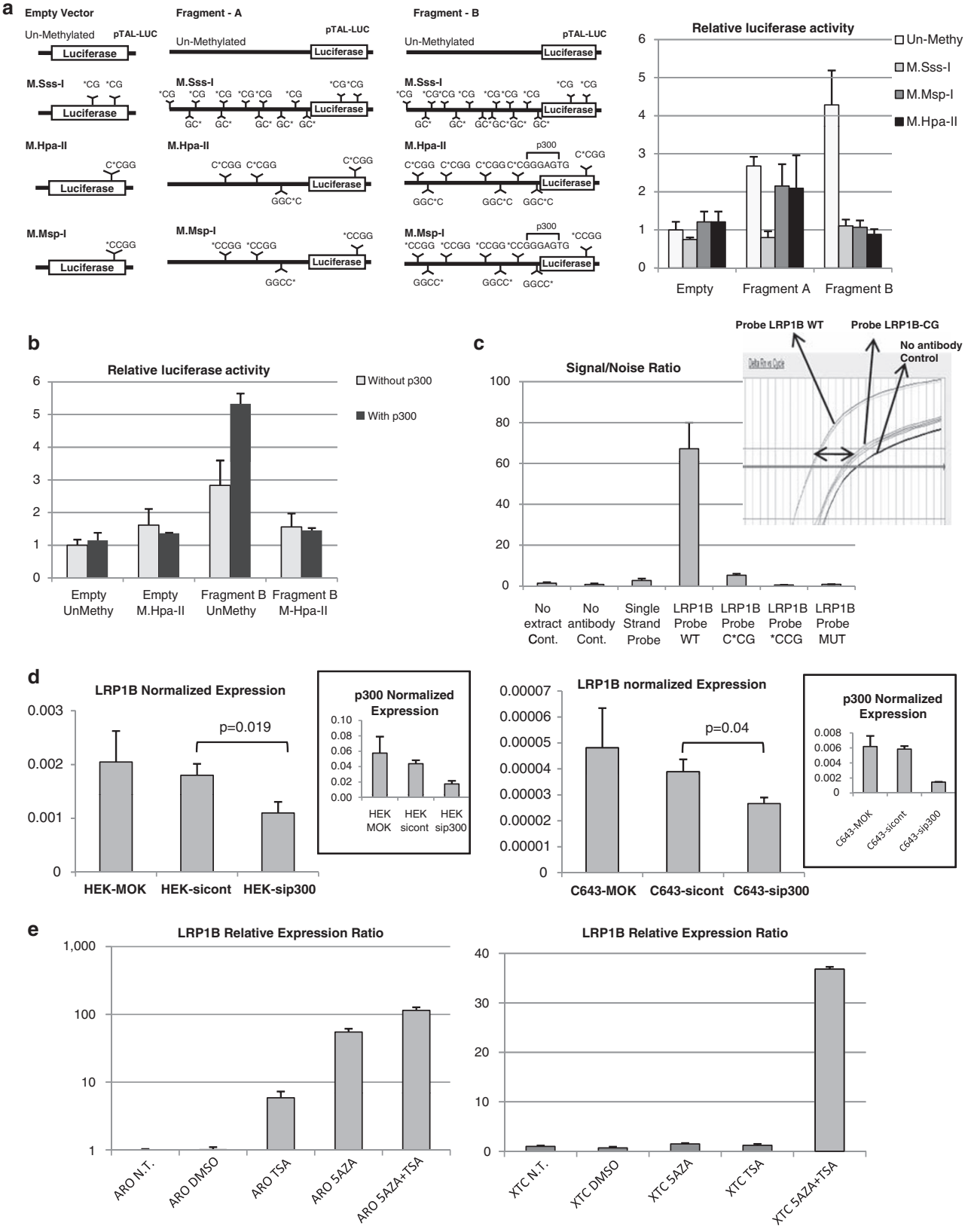
a
Empty Vector
Fragment - A
Fragment - B
Un-Methylated
pTAL-LUC
Luciferase
M.Sss-I
M.Hpa-II
M.Msp-I
Relative luciferase activity
Un-Methy
M.Sss-I
M.Msp-I
M.Hpa-II
Empty
Fragment A
Fragment B
b
Relative luciferase activity
Without p300
With p300
Empty UnMethy
Empty M.Hpa-II
Fragment B UnMethy
Fragment B M-Hpa-II
c
Signal/Noise Ratio
Probe LRP1B WT
Probe LRP1B-CG
No antibody Control
No extract Cont.
No antibody Cont.
Single Strand Probe
LRP1B Probe WT
LRP1B Probe C*CG
LRP1B Probe *CCG
LRP1B Probe MUT
d
LRP1B Normalized Expression
p=0.019
HEK-MOK
HEK-sicont
HEK-sip300
p300 Normalized Expression
HEK MOK
HEK sicont
HEK sip300
LRP1B normalized Expression
p=0.04
C643-MOK
C643-sicont
C643-sip300
p300 Normalized Expression
C643-MOK
C643-sicont
C643-sip300
e
LRP1B Relative Expression Ratio
ARO N.T.
ARO DMSO
ARO TSA
ARO 5AZA
ARO 5AZA+TSA
LRP1B Relative Expression Ratio
XTC N.T.
XTC DMSO
XTC 5AZA
XTC TSA
XTC 5AZA+TSA

tools. We selected 12 miRs by this *in silico* analysis (miR-155, −200b, −429, −548a, −548b, −548d, −520d, −524, −142, −7, −497 and miR-103). We quantified the expression of the 12 selected miRs in the 10 thyroid cancer cell lines available (see Supplementary Figure S4) and looked for miRs with an expression level that inversely correlated with LRP1B expression. By performing this sort of analysis, we could observe that overexpression of miR-548a-5p strikingly paralleled the decrease in LRP1B expression, with exception of the cell lines that previously demonstrated high levels of promoter methylation (ARO, KAT4 and XTC-1) (Figure 6a). This association was also observed *in vivo* in samples from the index fNMTC case. The miR-548a-5p binding site at LRP1B 3′UTR is conserved across six species, comprising primates, mice and chicken, and shows considerable sequence complementarity at the miR seed region (9-mers) (Figure 6b). Next, we proceeded to functionally validate that LRP1B is targeted by miR-548a-5p for downregulation. To examine whether miR-548a-5p binds to the 3UTR of LRP1B, we generated luciferase reporters encoding the wild-type and mutated versions of the LRP1B 3′UTR. We transfected HEK293 cells with an expression plasmid encoding the precursor transcript of miR-548a-5p (PremiR-548a-5p) and observed that overexpression of miR-548a-5p decreased the activity of the LRP1B 3′UTR luciferase reporter (Figure 6c). This effect was abrogated in the mutant LRP1B 3′UTR reporter, in which the binding site of miR-548a-5p was mutated (Figure 6c). To further support the relationship between LRP1B and miR-548a-5p, we employed anti-miR sequences to specifically inhibit miR-548a-5p expression in a cell line previously shown to have miR-548a-5p overexpression and very low levels of LRP1B (TPC-1). We verified that treatment with anti-miR-548a-5p, but not a scramble control, resulted in the increase of endogenous LRP1B mRNA levels (Figure 6d). miR-548a-5p is derived from processing of a pri-miR intergenic transcript, encoded by a minute inverted repeat transposable element, which maps to 8q22.3. Interestingly, 8q gains were one of the most frequent cytogenetic abnormalities in thyroid cancer cell lines (Ribeiro *et al*., 2008) and 8q22 amplification is a recurrent finding in several solid malignancies and may subclassify breast cancer patients with poor prognosis (Chin *et al*., 2007; Walker *et al*., 2008; Horlings *et al*., 2010). However, miRs in this location were always disregarded in surveys for genes upregulated in this amplified region. In the interest of exploring the hypothesis that DNA gains could be the key underlying mechanism of miR-548a-5p overexpression, we employed TaqMan Copy number assays (Applied Biosystems, Carlsbad, CA, USA) to ascertain DNA copy number at the miR-548a-5p *locus* (8q22.3). We found that 6/10 cell lines display copy number gains, whereas two cell lines display copy number loss (Figure 6e). Copy number gains at 8q22.3 are significantly correlated with miRNA-548a-3 overexpression (Figure 6f). These findings provide evidence for a novel mechanism of LRP1B inactivation, alternative to DNA methylation, acting through 8q22.3 genomic gain, miR-548a-5p overexpression and direct targeting of LRP1B. Integration of these 'hits' indicates that LRP1B inactivation may arise through diverse sequence of events during carcinogenesis (see Supplementary Table S3).

Restoration of LRP1B inhibits in vitro *and* in vivo *growth, and impairs matrigel cell invasion*

The role of LRP1B as a tumor suppressor is poorly studied. In keeping with the hypothesis that LRP1B acts as a tumor suppressor gene, we looked for a reversal of the malignant phenotype upon restoration of LRP1B. XTC-1 cells stably transfected with either a mini-receptor form of LRP1B (mLRP1B), which mimics the function and trafficking of LRP1B (Liu *et al*., 2001), or an empty vector were used in soft agar growth assays. We found that XTC-1 cells stably expressing mLRP1B gave rise to a significantly lower number of colonies as compared with cells selected with an empty vector ($P<0.05$, Figures 7a and b). To examine the effect of LRP1B in tumor growth *in vivo*, CHO cells, which are null for endogenous LRP1B, were stably transfected with either mLRP1B or empty vector and were inoculated into chicken chorioallantoic membrane. Six days after inoculation, all embryos developed tumors. However, tumors derived from mLRP1B-expressing cells were significantly smaller ($P=0.002$) than tumors derived from CHO cells transfected with the empty vector (Figures 7c and d). In order to determine the role of LRP1B in cancer cell

Figure 5 DNA methylation at a specific site of intron 1 of LRP1B disrupts binding and transcription enhancement mediated by p300. (**a**) Luciferase activity derived from transfection of HEK293 cells with pTAL-LUC reporter constructs containing independent fragments of the LRP1B CpG island (fragment A: −429 to −1 and fragment B: +1 to +530, counting from ATG), each subjected to *in vitro* methylation using M.Sss-I, M.Msp-I or M.Hpa-II (with *CG, *CCGG and C*CGG methylation specificities, respectively) as is represented schematically. (**b**) In the second experiment, luciferase activity of unmethylated and M.Hpa-II methylated constructs was measured in either the presence or the absence of a p300 expression vector co-transfected along with the reporters. (**c**) Proximity ligation real-time PCR quantification of the interactions between p300 and DNA probes consisting of the putative LRP1B p300 motif sequence in wild-type (WT), mutated (MUT) and methylated (C*CG and C*CG) configurations. The inset displays real-time PCR amplification curves. Results were expressed as signal/noise ratio, where the number of ligations in the sample was divided by the number of ligations in the negative control. (**d**) Expression of endogenous LRP1B upon inhibition of endogenous p300 by small interfering RNA (siRNA). HEK293 and C643 cells were transfected with a scramble siRNA control (siCont) or with a siRNA for p300 (sip300) and the effect on LRP1B expression was quantified by real-time PCR. The insets show concomitant underexpression of p300 in the same samples. The graphs integrate data from three experiments. (**e**) Analysis of LRP1B mRNA expression upon treatment of ARO and XTC-1 cell lines (displaying LRP1B CpG island DNA methylation) with 5AZA, TSA or both (5AZA + TSA). Non-treated cells (NT) or cells treated with dimethyl sulfoxide solvent were used as controls.

invasion, we performed *in vitro* matrigel invasion assays employing the otherwise highly invasive UTC cell line 8505C, in which mLRP1B was stably introduced. We observed a significant inhibition of invasive capacity of 8505C stably expressing mLRP1B relative to cells selected with the empty vector ($P<0.01$, Figure 7e).

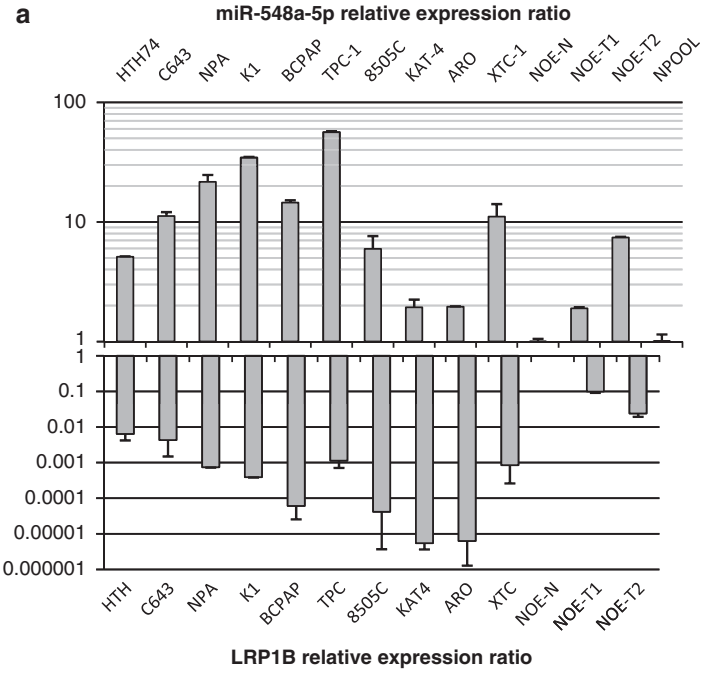

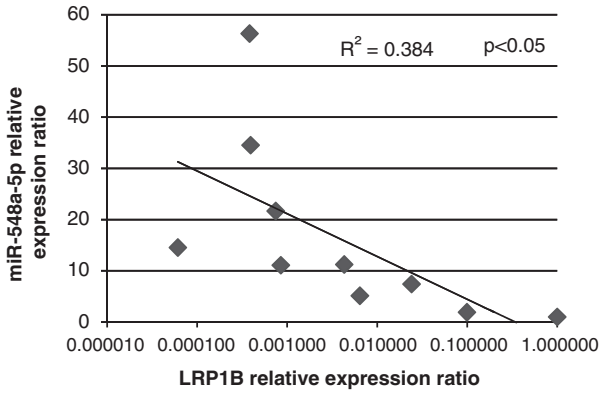

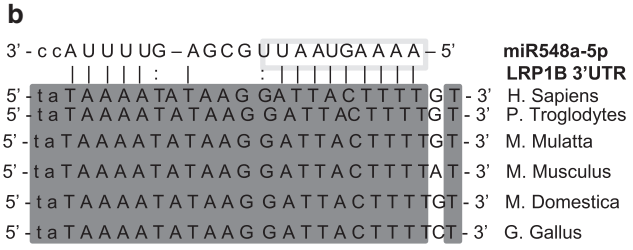

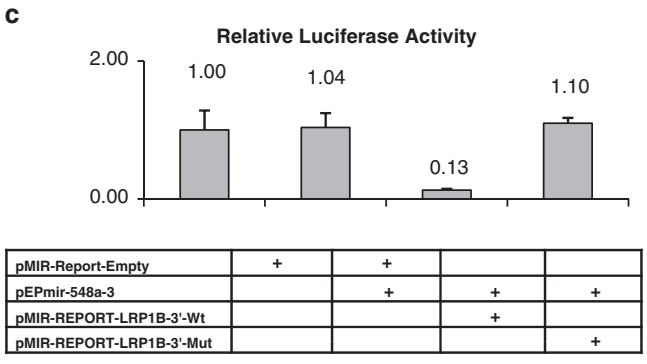

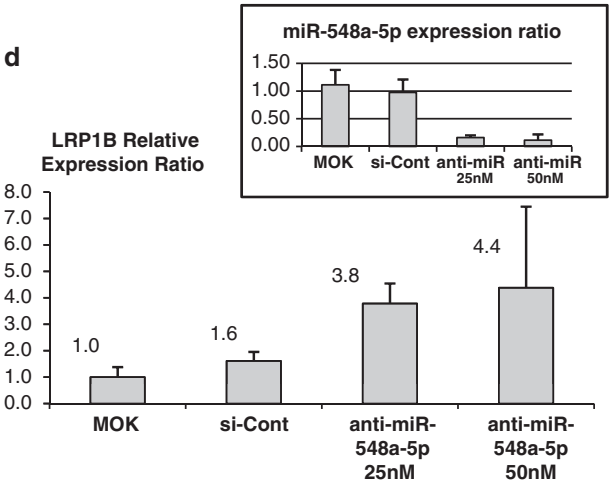

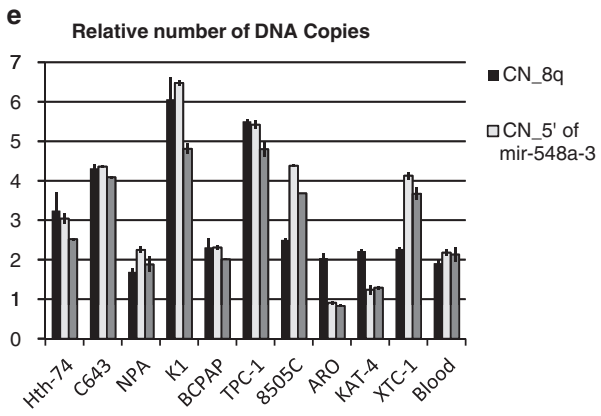

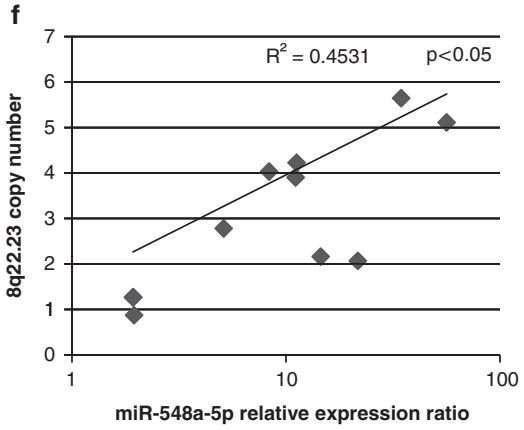

LRP1B leads to overall changes in the extracellular microenvironment

Working under the hypothesis that through its endocytic activity LRP1B might modulate the amount of soluble factors in the tumor microenvironment, we decided to investigate the impact of LRP1B in the extracellular medium. For this purpose, we used membrane-based cytokine antibody arrays to compare the levels of 51 ytokines (Supplementary Figure S5A) in the conditioned medium of 8505C cells transfected with mLRP1B, relative to cells selected with empty vector. We found overall changes in the amounts of several cytokines quantified by this method (Supplementary Figures S5B–D). The most prominently altered molecules were Ferritin, TACE, TRAILR2, NRG1-beta1, NrCAM, TREM1 and XEDAR, all found to be reduced in the media of mLRP1B-expressing cells (Supplementary Figures S5C and D). Furthermore, several MMPs were found to be weakly reduced in mLRP1B 8505C cells. Nevertheless, the antibody employed in the array does not discriminate between the active and inactive form of MMPs. To clear the relation between LRP1B and MMPs, we performed gelatin zymography with the conditioned medium of 8505C cells. The cells were plated onto fibronectin-coated plates so as to stimulate the expression of MMPs. We found that the levels of matrix metalloproteinase 2, mainly the latent form, but not MMP9 or MMP1 (latent or active), were significantly reduced in the conditioned medium of mLRP1B-expressing cells (Figure 7f). We confirmed that this difference was not attributable to different levels of matrix metalloproteinase 2 mRNA in 8505C-empty and 8505C-mLRP1B cells, as settled by qRT–PCR quantification (Figure 7f inset).

Discussion

Overall, the present work led to the identification of an otherwise unexpected mechanistic link between chromosomal changes (at 2q21 and 8q22.3), an epigenetic transcription factor (p300) and a specific miR (miR-548a-5p) in (de)regulation of LRP1B, which in turn restrains cancer cell growth and invasion by modulating the extracellular medium (Figure 8).

In the start of this study, *LRP1B* came to our attention because it was shown to be the only gene significantly targeted for downregulation within the 2q21 susceptibility *locus*, both in familial and in sporadic NMTC. Despite the lack of finding a causative germline mutation in the index family, at this point we cannot exclude *LRP1B* as a candidate gene for fNMTC. However, we do not disregard some weaknesses that might have arisen from our strategy. In one hand, the small size of the index family (a common feature in fNMTC) did not allow ascertainment of linkage to 2q21. Despite a high probability of a susceptibility *locus* at 2q21 existing on the basis of the pattern of allelic losses, focus on 2q21 without definitive evidence of linkage may have misled our search from alternative fNMTC *loci* reported at 14q (Bignell *et al*., 1997), 1q21 (Malchoff *et al*., 2000), 19p13.2 (Canzian *et al*., 1998), 8p23 (Cavaco *et al*., 2008), 8q24 (He *et al*., 2009), 1q21 and 6q22 (Suh *et al*., 2009). On the other hand, because the LRP1B coding sequence is 16 kbp long and consists of 91 exons, it was not feasible to perform exhaustive mutation screening in a larger set of samples. We are undertaking further sequencing efforts employing genome sequencing technology in a larger number of families linked to 2q21 in order to clear this issue.

Nevertheless, we were able to demonstrate somatic mutation and frequent genomic deletions involving LRP1B in sporadic non-medullary thyroid cancer, which, aside from thyroid cancer, are observed across various cancer types, namely in the lung, esophagus, breast, hepatocellular, renal, neural and colorectal cancer (http://www.broadinstitute.org/tumorscape/pages/portalHome.jsf).

Aside from structural alterations, we showed transcriptional silencing of LRP1B due to DNA methylation, disrupting a previously undisclosed functional

Figure 6 Overexpression of miR-548a-5p leads to LRP1B downregulation. (**a**) Correlation between miR-548a-5p expression and LRP1B mRNA levels in thyroid cancer cell lines, normal and tumor material from the index case (normal thyroid, fNMTC-tumor1 and fNMTC-tumor2). Alignment of the two graphics illustrates the tight inverse correlation between miR-548a-5p and LRP1B, which is observed both in cell lines and *in vivo* (fNMTC-tumor1 and -tumor2 samples). In cell lines ARO and KAT4, LRP1B is highly downregulated without simultaneous miR-548a-5p overexpression, which is probably the result of previously demonstrated alternative inactivation events such as copy number loss and complete promoter hypermethylation (Supplementary Table S3). The inverse correlation between miR-548a-5p and LRP1B was demonstrated by an X/Y plot with a significant Pearson correlation (ARO and KAT4 were excluded from this analysis). (**b**) Degree of sequence complementarity between miR-548a-5p seed region and its cognate binding site at the LRP1B 3′UTR (9-mers). This site is conserved among primate species, mice and chicken. (**c**) Luciferase activity was assayed in HEK293 cells co-transfected with a miR-548a-5p expression vector (pEPmir-548a-3) along with either a pMIR-REPORT construct containing the wild-type 3′UTR of LRP1B (pMIR-REPORT-LRP1B-3′-Wt) or a 3′UTR sequence in which two nucleotides of the miR-548a-5p seed region were mutated (pMIR-REPORT-LRP1B-3'-Mut). (**d**) Endogenous expression of LRP1B upon 16 h treatment of TPC-1 cells with anti-miR-548a-5p RNAs in two concentrations: 25 nM and 50 nM. A scramble control siRNA (siCont) and mock (MOK) conditions were used as controls. The inset shows concomitant underexpression of miR-548a-5p in the same samples. The graph integrates data from three experiments. (**e**) Analysis of miR-548a-3 DNA copy number in thyroid cancer cell lines determined by genomic quantitative real-time PCR employing primer/probe pairs targeting genetic regions immediately upstream and downstream of the miR-548a-5p genomic *locus* (CN_5′ of miR-548a-3 and CN_3'of miR-548a-3) as well as at a region near the 8q centromere (CN_8q). The abundance of DNA copies at each site was normalized to an endogenous control for RNAse P run in multiplex reactions and copy number values were calibrated by performing reactions with blood-derived DNA sample in the same plate. Data were generated with the CopyCaller software. (**f**) Correlation between DNA copy number at the miR-548a-5p *locus* and miR-548a-5p expression.

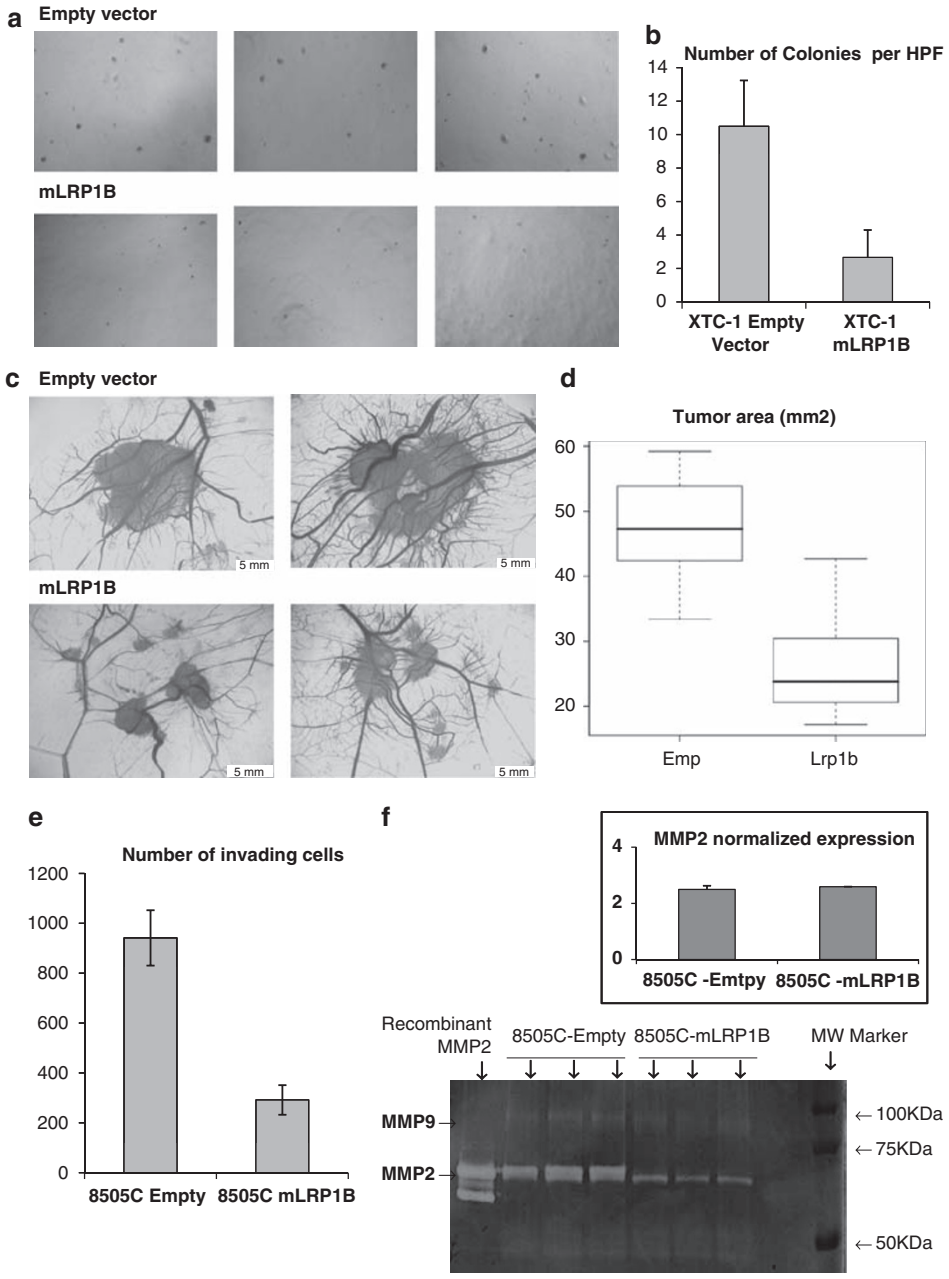

Figure 7 LRP1B inhibits *in vitro* and *in vivo* tumor growth, impairs *in vitro* cell invasion and leads to a reduction of matrix metalloproteinase 2 (MMP2) in the extracellular medium. (**a**) Soft agar growth was measured in XTC-1 cells stably selected with either an expression vector encoding a LRP1B mini-receptor, which mimics the function and trafficking of LRP1B (mLRP1B), or an empty vector control (empty vector). The XTC-1 cell line was chosen on the basis that it forms agar colonies and because endogenous LRP1B mRNA was greatly impaired. Stable clones were pooled and 5000 cells per well were mixed with soft agar in appropriate medium and plated in six-well plates previously coated with a bottom layer of agar. (**b**) After 2 weeks in the incubator, colonies were stained with crystal violet, photographed and counted. (**c**) *In vivo* chicken embryo growth assay was performed using CHO cells stably transfected with either mLRP1B or empty vector control. A total of 2×10^6 cells were inoculated into the chorioallantoic membrane and allowed to grow for 6 days. The resulting tumors were photographed. (**d**) *Ex ovo* images were used to determine the areas of the tumors and produce a box plot, which integrates data from seven different inoculations of each condition. The Wilcoxon rank sum test was used to calculate statistical significance. (**e**) *In vitro* cell invasion assayed by matrigel invasion chambers in 8505C cells stably transfected with mLRP1B or empty vector control. A total of 2.5×10^4 cells were plated in 24-well plates with filter inserts containing a polyethylene terephthalate membrane of 8 μm size pores occluded by a thin layer of matrigel basement membrane matrix. After 24 h, the invasive cells that were able to invade into the lower surface of the filter were fixed, stained with DAPI and counted under the microscope. The graph contains data from three experiments. (**f**) Conditioned medium was obtained from stable 8505C mLRP1B or 8505C empty vector control cells by placing 2.5×10^5 cells in fibronectin-coated six-well plates for 24 h in 1 ml serum-free media. Three wells were seeded for each condition (triplicates). For gelatin zymography, 20 μl of the same conditioned medium was separated in a non-reducing PAGE gel containing 1 mg/ml gelatin. After MMP activation, gels were stained with Coomassie blue to allow the visualization of gelatinolytic bands. This experiment was performed twice and a representative gel is presented. Recombinant MMP2 was used as a control. Low-molecular-weight bands in the control were generated by MMP2 autolysis.

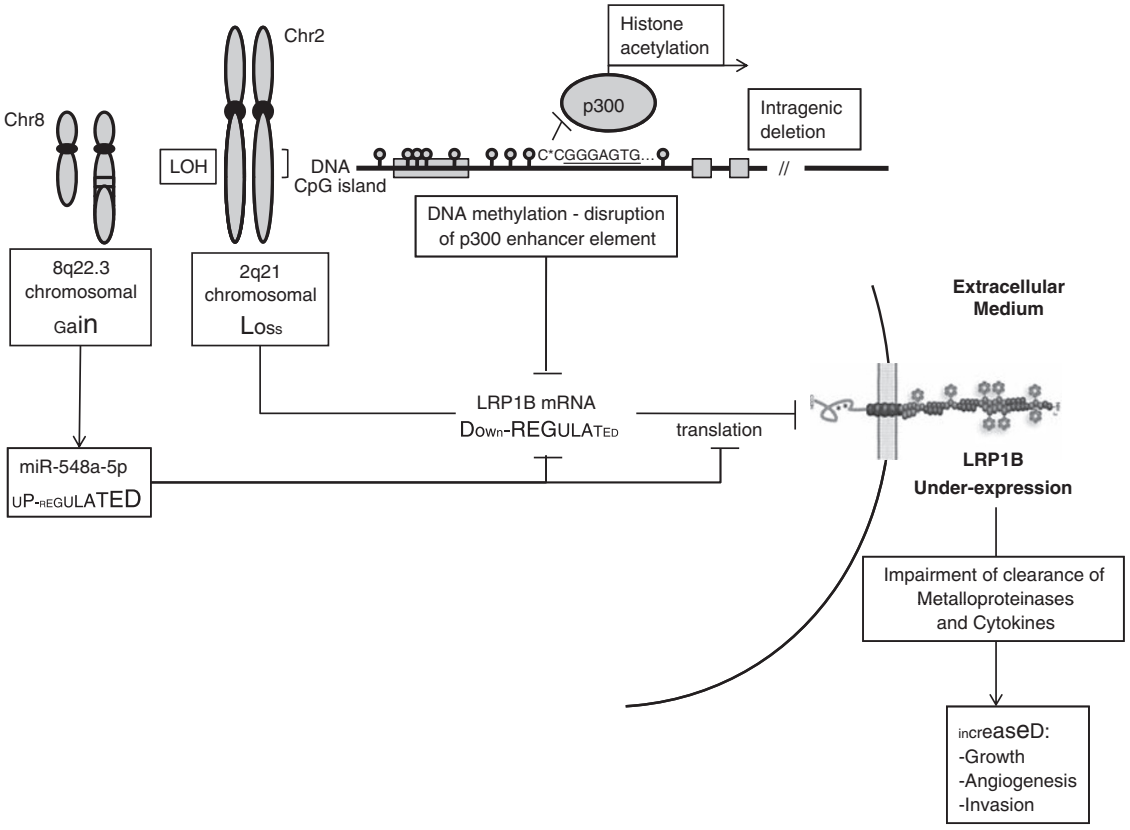

Figure 8 Schematic representation of chromosomal, epigenetic and microRNA-mediated changes leading to LRP1B (de)regulation, which, in turn, restrains cancer cell growth and invasion by mediating clearance of matrix metalloproteinase 2 from the extracellular medium.

p300 binding site at intron 1 of LRP1B. The EP300 gene encodes p300, a histone-acetyltransferase that regulates transcription via chromatin remodeling, and is important in the processes of cell proliferation and differentiation (Gayther *et al*., 2000). A role for p300 in cancer has been previously implied by the fact that it is targeted by viral oncoproteins (Arany *et al*., 1995), it is fused to myeloid lymphoblastic leukemia in leukemia (Ida *et al*., 1997) and mutations in EP300 were described in epithelial malignancies with inactivation of the second allele (Muraoka *et al*., 1996; Gayther *et al*., 2000). Our results are of significance as they place LRP1B in the p300 suppressor pathway.

In this work, we have noticed that genomic gain at 8q22.3 goes together with miR-548a-5p overexpression, which in turn directly targets LRP1B for downregulation, resulting in increased invasive capacity. Chromosome 8q22 amplification has been repeatedly associated with poor patient outcome in other cancer models, particularly in breast cancer (Chin *et al*., 2007; Walker *et al*., 2008; Horlings *et al*., 2010). It remains to be seen whether poor patient outcome is due to the workings of this newly identified circuitry.

At some point in epithelial tumor progression, cancer cells overcome the basement membrane and acquire the means to invade through the interstitial connective tissue. These properties are partly conferred by activating proteolysis systems, which promote extracellular matrix degradation such as the uPA (Ulisse *et al*., 2009) and MMPs (Roy *et al*., 2009). Aside from modulating matrix metalloproteinase 2, as shown here, LRP1B has also been reported to regulate the uPA system (Liu *et al*., 2001). Cells expressing LRP1B display a substantially slower rate of uPA/plasminogen activator inhibitor type-1 complex internalization (Knisely *et al*., 2007), which impairs the regeneration of unoccupied urokinase plasminogen activator receptor on the cell surface and correlates with a diminished rate of cell migration (Li *et al*., 2002; Tanaga *et al*., 2004). Our results highlight LRP1B as an unconventional and yet key tumor suppressor acting as a regulator of the 'extracellular proteome' and constraining the abundance of critical members of proteolytic systems in the tumor microenvironment. These functions may be overlapping and yet distinct from other LDL receptor family members (Liu *et al*., 2001). The closest related member, LRP1, shows controversial effects on MMP catabolism and cell invasion, which seem to be dependent on the cell context (Hahn-Dantona *et al*., 2001; Yang *et al*., 2001; Emonard *et al*., 2004; Desrosiers *et al*., 2006; Dedieu *et al*., 2008; Song *et al*., 2009).

As the extracellular domain of LRP1B may potentially bind to a myriad of still undisclosed ligands (Marschang *et al*., 2004), it is possible that the tumor suppressor properties of this receptor are further explained by modulation of the extracellular concentration of other molecules critical for tumor progression, secreted by cancer cells originating from other types of cancers.

It is also conceivable that additional tumor suppressor functions of LRP1B are mediated by signaling pathways elicited by its intracellular domain (Liu *et al*., 2007; Shiroshima *et al*., 2009).

Our findings give scope for the use of LRP1B activity as a tool for a therapeutic approach that is not centered on the cancer cell itself, but rather in its environment, aiming to control the invasive behavior of the cancer cell by modulating the composition of the environment surrounding it. This may have repercussions to some of the most prevalent cancer types in which LRP1B is also found to be silenced (Supplementary Figure S6). A future challenge will be to use the newly identified LRP1B (de)regulatory mechanisms to design the strategy for such intervention.

Materials and methods

Familial subjects
The index fNMTC family studied was reported elsewhere (Prazeres *et al*., 2008) and the pedigree is depicted in Supplementary Figure S1A.

Sporadic cases
The testing series consisted of 71 formalin-fixed, paraffin-embedded tissue samples, comprising 20 FTAs, 17 FTCs, 24 PTCs and 10 undifferentiated thyroid carcinomas (UTCs). We also studied 24 samples of normal thyroid tissue dissected from specimens obtained from total thyroidectomies.

Cell lines and transfections
We used 10 cell lines, HTH74, C643, NPA, K1, BCPAP, TPC-1, 8505C, KAT4, ARO and XTC-1, otherwise reported to be derived from thyroid cancer. However, during the course of this work, Schweppe *et al*. (2008) performed short tandem repeat and single-nucleotide polymorphism analysis of several thyroid cancer cell lines and suggested that cell lines ARO and KAT4 may be derivates of the HT-29 colon cancer cell line. Also, NPA was suggested to be a derivative of the M14/MDA-MB-435S melanoma cell line.

The above-mentioned 10 cell lines were maintained in RPMI medium, supplemented with 10% fetal bovine serum, 100 μg/ml streptomycin and 100 U/ml penicillin, in a humidified atmosphere, with 5% CO_2, at 37 °C. The cell line HEK293 was maintained in Dulbecco's modied Eagle's medium with 10% fetal bovine serum and 100 μg/ml penicillin/streptomycin. HEK293 cells, used primarily for reporter assays, were transfected by the calcium phosphate method. Transfection of the remaining cell lines was achieved using Lipofectamin Reagent (Invitrogen, Carlsbad, CA, USA).

Microarray global gene expression analysis
Tissue samples collected immediately after surgical resection were directly put into TRIZOL (Ambion Inc., Austin, TX, USA) and immediately homogenized. RNA was extracted according to the TRIZOL protocol and further clean-up was achieved by passing RNA through an RNeasy column (Qiagen, Hilden, Germany). Complementary RNA was synthesized by reverse transcriptase–PCR using an oligo dT primer with a T7 promoter overhang followed by *in vitro* transcription. Complementary RNA was labeled by incorporating biotinylated nucleotides. The complementary RNA target was fragmented and hybridized to the HG U133 Plus 2.0 genechip (Affymetrix). After staining and image acquisition, the signal intensity data were normalized by the invariant probeset method and the expression values were computed using the dChip software (Cheng Li Lab, http://biosun1.harvard.edu/complab/dchip/).

mRNA expression
RNA was obtained from macrodissected 4×20 μm tissue sections with the RecoverAll RNA Isolation Kit (Ambion). RNA from cell lines was purified by the TRIZOL protocol. After cDNA synthesis employing MMLV Reverse Transcriptase (Applied Biosystems), TaqMan Gene Expression assay hs-00218582_m1 was used to measure LRP1B expression, matrix metalloproteinase 2 was assayed by TaqMan hs00234422_m1 qRT–PCR experiments. A normal reference was produced by pooling RNAs from nine samples of normal thyroid tissue, treated in the same way as the tumor samples. Data were analyzed by the absolute quantification method.

Validation series
A validation set of cases, gathered by an independent group, consisted of 30 thyroid lesions (12 FTAs and 18 FTCs) and 12 specimens of normal thyroid tissue, which were independently assessed for LRP1B expression by analyzing the data concerning the LRP1B probesets represented in the GeneChip Human Exon 1.0 ST Array (Affymetrix). Thyroid samples were collected immediately after surgical resection, snapped frozen and stored at −80 °C. All samples were visually inspected on 5 μm hematoxylin and eosin-stained frozen sections by the pathologist (JC-T). Cryostat sections were disrupted by using a Polytron homogeneizer (Glen Mills Inc., Clifton, NJ, USA) and total RNA was isolated from cryostat sections using RNeasy Mini Kit (Qiagen) following the manufacturer's instructions. RNA quality was assessed on a bioanalyser (Agilent Technologies) and samples with RIN (RNA integrity number) >7.0 were used for array experiments. In total, 1 μg of the total RNA was used for rRNA reduction, synthesis, fragmentation and labeling following the standard Affymetrix Whole-Transcript Sense Target-Labeling Assay protocol. Each thyroid sample was hybridized with an Affymetrix Human Exon 1.0 ST microarray. Background correction, normalization, probe summarization and data analysis were done with Partek Genomics Suite software (Parket Incorporated, St Louis, MO, USA) using rate monotonic algorithm.

LRP1B mutation analysis
We designed 91 sets of PCR primers, which resulted in the amplification of flanking intronic boundaries and coding sequences of the 91 exons of LRP1B. We also used a set of 11 exonic primer pairs in order to amplify cDNA fragments ranging from 1 to 1.4 kbp encompassing several exons. PCR products were directly sequenced. Primer sequences are available upon request.

Copy number analysis
We used TaqMan Copy number assay (Applied Biosystems) in order to estimate the copy number at several genomic locations within LRP1B, namely at exons 5 (assay hs-02812600_cn), 44 (assay hs-02217633_cn) and 90 (assay hs-05832428_cn), and also near the centromeric region of chromosome 2q (assay hs-04631472_cn). A similar strategy was used to determine copy number at the genomic location of miR-548a-3 (assays hs-05036789_cn and hs-06224496_cn) and at proximity of the 8q centromere (assay hs-06217400_cn). Multiplex genomic

qRT–PCR reactions, containing VIC-TaqMan-primer/probes for an internal reference gene (RNAse P) and FAM-labeled TaqMan-primer/probes for the interrogated location, were performed in triplicates. Results were analyzed with the CopyCaller software (Applied Biosystems). DNA copy number was calibrated by using a blood sample run in the same plate.

DNA methylation analysis

Genomic DNA was converted by bisulfite treatment using the Epitect modification kit (Qiagen) and subsequently subjected to PCR amplification of two regions of the promoter: fragment 1 (−131 to +100, from ATG) and fragment 2 (+217 to +365). The bisulfite PCR products were directly sequenced.

Constructs and expression vectors

5′CpG island reporter constructs. Two fragments of the LRP1B CpG island, obtained by PCR amplification of nucleotides −429 to −1 from the ATG (fragment A) and of nucleotides +1 to +530 (fragment B), were ligated into the pTAL-LUC vector (ClonTech, Mountain View, CA, USA), encoding the firefly luciferase gene under a basic TATA-like promoter region of the herpes simplex virus thymidine kinase promoter.

In vitro *methylation using bacterial methyltransferases*. Bacterial methyltransferases with distinct specificities, M.Sss-I, M.Hpa-II and M.Msp-I (methylating at *CG, C*CGG and *CCGG, respectively), were used to methylate the CpG island constructs *in vitro*. Methylation reactions were set up by incubating 2 μg of plasmid DNA with 10 units of methyltransferase, in the presence of S-adenosylmethionine, at 37 °C, overnight. After *in vitro* methylation, reporters were characterized by bisulfite sequencing.

3′UTR reporter constructs. We inserted a 645-bp sequence of the 3′ untranslated region (3′UTR) of LRP1B containing the miRNA-548a-3 target site downstream of the firefly luciferase reporter in the pMIR-Report vector (Ambion). By PCR, we generated both wild-type and a mutant version of the 3′UTR in which two nucleotides from the target sequence complementary to the seed region of miRNA-548a-3 were mutated.

Expression vectors. A pCDNA3.0 vector expressing an LRP1B mini-receptor (mLRP1B) comprised of the entire cytoplasmatic tail, the trans-membrane region and extracellular sub-domain IV, which mimics the function and trafficking of LRP1B, was kindly provided by Dr Guojun Bu. An expression vector encoding the pre-miR-548a-5p (pEP-mir-548a-3) was purchased from Cell Biolabs (Cell Biolabs Inc., San Diego, CA, USA). A pCMV-β vector expressing the p300 histone-acetyltransferase was obtained from Dr William Sellers, through Addgene (Addgene plasmid 10718).

Reporter assays. DNA mixtures consisted of 0.5 μg expression plasmid, 0.5 μg of the reporter plasmid, 0.5 μg of PDM2-LacZ (expressing β-galactosidase) and pUC18, to complete 5 μg total DNA. Cells were incubated with calcium phosphate–DNA complexes for 24 h and cultured in fresh medium for an additional 24–48 h. Cells were harvested and lysed in 150 μl of reporter lysis buffer, and luciferase and β-galactosidase assays were performed. The luciferase activity was normalized with the corresponding β-Galactosidase activity (measures transfection efficiency). All conditions were performed in triplicates and experiments were performed three times.

Proximity ligation assay. Analysis of the interaction between DNA and p300 was performed by a proximity ligation assay as described by Gustafsdottir *et al*. (2007), with the following modifications:

(1) The variable region of the DNA probe was designed to have 24 nucleotides encompassing the predicted p300 binding site at LRP1B intron 1 in the wild-type (CCCCTCCGGG AGTGTGTGCACTTG) and mutated (CCCCTCCGGGACA GTGTGCACTTG) configurations, as well as with methylated sites (CCCCTC*CGGGAGTGTGTGCACTTG and CCCCT* CCGGGAGTGTGTGCACTTG, where '*C' represents the sites where a 5-methyl cytosine modification was introduced). The variable part of the probes was made double-stranded by hybridizing an equimolar amount of a complementary 24-mer oligonucleotide in which the methylation sites were placed in the symmetrical positions. Probes were synthesized at MWG Eurofins (Eurofins MWG Operon, Ebersberg, Germany).

(2) Proximity ligation reactions were set up in a p300 binding buffer described by Rikitake and Moran (1992). Then, a p300 biotinylated antibody (R&D Systems, Minneapolis, MN, USA) conjugated with streptavidin-oligonucleotide probes (kindly provided by Sigurn Gustafsdottir) was added and the mixture was incubated for 4 h at 4 °C.

Treatment of cells with 5AZA and TSA. A total of 1×10^5 cells per well were seeded, in triplicates, in six-well-chambers. The next day, cells were cultured in a medium containing either regular medium, or medium supplemented with dimethyl sulfoxide solvent or 5 μM 5AZA (Sigma-Aldrich, St Louis, MO, USA). Medium corresponding to each formulation was renewed daily for 4 days, after which nucleic acids were extracted. Treatment with TSA alone was performed by adding 100 nM of TSA to the medium for 16 h. For the combination of 5AZA with TSA, 100 nM TSA (Sigma) was added at the fourth day of the 5AZA treatment and kept for 16 h, after which the experiment was stopped.

Quantification of miRs. miRNAs were quantified using TaqMan MicroRNA Assays (Applied Biosystems). Starting from 10 ng of total RNA, primer-specific reverse transcription was performed and 2 μl of cDNA was used in qRT–PCR to quantify each miR. Expression values were normalized to the levels of miRNA-U6b determined in the same RNA samples. A pool of nine RNAs derived from normal thyroid tissue was used as the normal reference. Data were analyzed using the delta-delta-Ct method.

Soft agar assays. For soft agar assays, we prepared plates containing a bottom layer of 0.7% agar in Dulbecco's modied Eagle's medium, 10% fetal bovine serum, 1% penicillin/streptomicin and 5000 cells were diluted in 2× Dulbecco's modied Eagle's medium, 20% fetal bovine serum, 2% penicillin/streptomycin P, mixed with equal volume of 1% agar at 40 °C and plated on the agar plates. After 2–3 weeks, wells were stained with crystal violet and colonies were photographed and counted.

Chicken embryo in vivo *growth assay*. The chicken embryo chorioallantoic membrane model has been used to assay tumorigenicity as previously described (Hagedorn *et al*., 2005) with minor modifications, which consisted of placement of a nylon ring with 5 mm diameter on top of the growing chicken chorioallantoic membrane under sterile conditions for adding 2×10^6 per embryo.

In vitro *matrigel invasion assays*. Matrigel Invasion Chambers (BD Biosciences, Franklin Lakes, NJ, USA) were used to assess the *in vitro* metastatic potential according to reported procedures (Mateus *et al*., 2009).

Gelatin zymography. The level of gelatinases was determined as described by others (Ribeiro *et al*., 2010) in 24-h conditioned medium derived from 2.5×10^5 cells seeded onto six-well plates previously coated with 20 μg/ml fibronectin. The experiment was performed in triplicates (three wells for each condition) and was repeated twice.

Statistical analyses
Differences between groups were tested by the Mann–Whitney test. Correlations were assessed by the Pearson coefficient.

Abbreviations

fNMTC, familial non-medullary thyroid cancer; FTA, follicular thyroid adenoma; FTC, follicular thyroid carcinoma; LRP1B, low-density lipoprotein receptor-related protein; miR, microRNA; mLRP1B, LRP1B minireceptor; NMTC, non-medullary thyroid cancer; PTC, papillary thyroid carcinoma; qRT–PCR, quantitative real-time PCR; TSA, trichostatin A; uPA, urokinase plasminogen activator; UTC, undifferentiated thyroid carcinoma; 5AZA, 5-aza-2′-deoxycytidine.

Conflict of interest

The authors declare no conflict of interest.

Acknowledgements

We would like to acknowledge funding from grants from the Portuguese Foundation for Science and Technology (SFRH/BD30041/2006 and PTDC/SAU-OBD/101242/2008), the Portuguese Society of Endocrinology and Metabolism (Edward Limber Prize) and the Portuguese Ministry of Health (project 13/2007). José Cameselle-Teijeiro was supported by Grant PS09/02050-FEDER, from the Ministry of Science and Innovation (Instituto de Salud Carlos III), Spain. IPATIMUP is an associated laboratory of the Portuguese Ministry of Science, Technology and Higher Education and is partially supported by the Portuguese Foundation for Science and Technology.

References

Arany Z, Newsome D, Oldread E, Livingston DM, Eckner R. (1995). A family of transcriptional adaptor proteins targeted by the E1A oncoprotein. *Nature* **374**: 81–84.

Asami Y, Mori M, Koshino H, Sekiyama Y, Teruya T, Simizu S *et al*. (2009). A cell-based screening to detect inhibitors of BRAF signaling pathway. *J Antibiot (Tokyo)* **62**: 105–107.

Beroukhim R, Mermel CH, Porter D, Wei G, Raychaudhuri S, Donovan J *et al*. (2010). The landscape of somatic copy-number alteration across human cancers. *Nature* **463**: 899–905.

Bignell GR, Canzian F, Shayeghi M, Stark M, Shugart YY, Biggs P *et al*. (1997). Familial nontoxic multinodular thyroid goiter locus maps to chromosome 14q but does not account for familial nonmedullary thyroid cancer. *Am J Hum Genet* **61**: 1123–1130.

Canzian F, Amati P, Harach HR, Kraimps JL, Lesueur F, Barbier J *et al*. (1998). A gene predisposing to familial thyroid tumors with cell oxyphilia maps to chromosome 19p13.2. *Am J Hum Genet* **63**: 1743–1748.

Cavaco BM, Batista PF, Sobrinho LG, Leite V. (2008). Mapping a new familial thyroid epithelial neoplasia susceptibility locus to chromosome 8p23.1-p22 by high-density snp genome-wide linkage analysis. *J Clin Endocrinol Metab* **93**: 4426–4430.

Chin SF, Teschendorff AE, Marioni JC, Wang Y, Barbosa-Morais NL, Thorne NP *et al*. (2007). High-resolution aCGH and expression profiling identifies a novel genomic subtype of ER negative breast cancer. *Genome Biol* **8**: R215.

Clark SJ, Harrison J, Frommer M. (1995). CpNpG methylation in mammalian cells. *Nat Genet* **10**: 20–27.

Dedieu S, Langlois B, Devy J, Sid B, Henriet P, Sartelet H *et al*. (2008). LRP-1 silencing prevents malignant cell invasion despite increased pericellular proteolytic activities. *Mol Cell Biol* **28**: 2980–2995.

Desrosiers RR, Rivard ME, Grundy PE, Annabi B. (2006). Decrease in LDL receptor-related protein expression and function correlates with advanced stages of Wilms tumors. *Pediatr Blood Cancer* **46**: 40–49.

Emonard H, Bellon G, de Diesbach P, Mettlen M, Hornebeck W, Courtoy PJ. (2005). Regulation of matrix metalloproteinase (MMP) activity by the low-density lipoprotein receptor-related protein (LRP). A new function for an 'old friend'. *Biochimie* **87**: 369–376.

Emonard H, Bellon G, Troeberg L, Berton A, Robinet A, Henriet P *et al*. (2004). Low density lipoprotein receptor-related protein mediates endocytic clearance of pro-MMP-2.TIMP-2 complex through a thrombospondin-independent mechanism. *J Biol Chem* **279**: 54944–54951.

Gayther SA, Batley SJ, Linger L, Bannister A, Thorpe K, Chin SF *et al*. (2000). Mutations truncating the EP300 acetylase in human cancers. *Nat Genet* **24**: 300–303.

Gustafsdottir SM, Schlingemann J, Rada-Iglesias A, Schallmeiner E, Kamali-Moghaddam M, Wadelius C *et al*. (2007). *In vitro* analysis of DNA-protein interactions by proximity ligation. *Proc Natl Acad Sci USA* **104**: 3067–3072.

Hagedorn M, Javerzat S, Gilges D, Meyre A, de Lafarge B, Eichmann A *et al*. (2005). Accessing key steps of human tumor progression *in vivo* by using an avian embryo model. *Proc Natl Acad Sci USA* **102**: 1643–1648.

Hahn-Dantona E, Ruiz JF, Bornstein P, Strickland DK. (2001). The low density lipoprotein receptor-related protein modulates levels of matrix metalloproteinase 9 (MMP-9) by mediating its cellular catabolism. *J Biol Chem* **276**: 15498–15503.

He H, Nagy R, Liyanarachchi S, Jiao H, Li W, Suster S *et al*. (2009). A susceptibility locus for papillary thyroid carcinoma on chromosome 8q24. *Cancer Res* **69**: 625–631.

Heinemeyer T, Wingender E, Reuter I, Hermjakob H, Kel AE, Kel OV *et al*. (1998). Databases on transcriptional regulation: TRANSFAC, TRRD and COMPEL. *Nucleic Acids Res* **26**: 362–367.

Herz J, Clouthier DE, Hammer RE. (1992). LDL receptor-related protein internalizes and degrades uPA-PAI-1 complexes and is essential for embryo implantation. *Cell* **71**: 411–421.

Herz J, Strickland DK. (2001). LRP: a multifunctional scavenger and signaling receptor. *J Clin Invest* **108**: 779–784.

Horlings HM, Lai C, Nuyten DS, Halfwerk H, Kristel P, van Beers E *et al*. (2010). Integration of DNA copy number alterations and prognostic gene expression signatures in breast cancer patients. *Clin Cancer Res* **16**: 651–663.

Ida K, Kitabayashi I, Taki T, Taniwaki M, Noro K, Yamamoto M *et al*. (1997). Adenoviral E1A-associated protein p300 is involved in acute myeloid leukemia with t(11;22)(q23;q13). *Blood* **90**: 4699–4704.

Knisely JM, Li Y, Griffith JM, Geuze HJ, Schwartz AL, Bu G. (2007). Slow endocytosis of the LDL receptor-related protein 1B: implications for a novel cytoplasmic tail conformation. *Exp Cell Res* **313**: 3298–3307.

Kohno T, Otsuka A, Girard L, Sato M, Iwakawa R, Ogiwara H *et al*. (2010). A catalog of genes homozygously deleted in human lung cancer and the candidacy of PTPRD as a tumor suppressor gene. *Genes Chromosomes Cancer* **49**: 342–352.

Li Y, Knisely JM, Lu W, McCormick LM, Wang J, Henkin J *et al*. (2002). Low density lipoprotein (LDL) receptor-related protein 1B impairs urokinase receptor regeneration on the cell surface and inhibits cell migration. *J Biol Chem* **277**: 42366–42371.

Lister R, Pelizzola M, Dowen RH, Hawkins RD, Hon G, Tonti-Filippini J *et al*. (2009). Human DNA methylomes at base resolution show widespread epigenomic differences. *Nature* **462**: 315–322.

Liu CX, Li Y, Obermoeller-McCormick LM, Schwartz AL, Bu G. (2001). The putative tumor suppressor LRP1B, a novel member of the low density lipoprotein (LDL) receptor family, exhibits both overlapping and distinct properties with the LDL receptor-related protein. *J Biol Chem* **276**: 28889–28896.

Liu CX, Musco S, Lisitsina NM, Forgacs E, Minna JD, Lisitsyn NA. (2000a). LRP-DIT, a putative endocytic receptor gene, is frequently inactivated in non-small cell lung cancer cell lines. *Cancer Res* **60**: 1961–1967.

Liu CX, Musco S, Lisitsina NM, Yaklichkin SY, Lisitsyn NA. (2000b). Genomic organization of a new candidate tumor suppressor gene, LRP1B. *Genomics* **69**: 271–274.

Liu CX, Ranganathan S, Robinson S, Strickland DK. (2007). gamma-Secretase-mediated release of the low density lipoprotein receptor-related protein 1B intracellular domain suppresses anchorage-independent growth of neuroglioma cells. *J Biol Chem* **282**: 7504–7511.

Malchoff CD, Sarfarazi M, Tendler B, Forouhar F, Whalen G, Joshi V *et al*. (2000). Papillary thyroid carcinoma associated with papillary renal neoplasia: genetic linkage analysis of a distinct heritable tumor syndrome. *J Clin Endocrinol Metab* **85**: 1758–1764.

Malone CS, Miner MD, Doerr JR, Jackson JP, Jacobsen SE, Wall R *et al*. (2001). CmC(A/T)GG DNA methylation in mature B cell lymphoma gene silencing. *Proc Natl Acad Sci USA* **98**: 10404–10409.

Marschang P, Brich J, Weeber EJ, Sweatt JD, Shelton JM, Richardson JA *et al*. (2004). Normal development and fertility of knockout mice lacking the tumor suppressor gene LRP1b suggest functional compensation by LRP1. *Mol Cell Biol* **24**: 3782–3793.

Mateus AR, Simoes-Correia J, Figueiredo J, Heindl S, Alves CC, Suriano G *et al*. (2009). E-cadherin mutations and cell motility: a genotype-phenotype correlation. *Exp Cell Res* **315**: 1393–1402.

May P, Woldt E, Matz RL, Boucher P. (2007). The LDL receptor-related protein (LRP) family: an old family of proteins with new physiological functions. *Ann Med* **39**: 219–228.

McKay JD, Lesueur F, Jonard L, Pastore A, Williamson J, Hoffman L *et al*. (2001). Localization of a susceptibility gene for familial nonmedullary thyroid carcinoma to chromosome 2q21. *Am J Hum Genet* **69**: 440–446.

Muraoka M, Konishi M, Kikuchi-Yanoshita R, Tanaka K, Shitara N, Chong JM *et al*. (1996). p300 gene alterations in colorectal and gastric carcinomas. *Oncogene* **12**: 1565–1569.

Nagel R, le Sage C, Diosdado B, van der Waal M, Oude Vrielink JA, Bolijn A *et al*. (2008). Regulation of the adenomatous polyposis coli gene by the miR-135 family in colorectal cancer. *Cancer Res* **68**: 5795–5802.

Nykjaer A, Petersen CM, Moller B, Jensen PH, Moestrup SK, Holtet TL *et al*. (1992). Purified alpha 2-macroglobulin receptor/LDL receptor-related protein binds urokinase.plasminogen activator inhibitor type-1 complex. Evidence that the alpha 2-macroglobulin receptor mediates cellular degradation of urokinase receptor-bound complexes. *J Biol Chem* **267**: 14543–14546.

Prazeres HJ, Rodrigues F, Soares P, Naidenov P, Figueiredo P, Campos B *et al*. (2008). Loss of heterozygosity at 19p13.2 and 2q21 in tumours from familial clusters of non-medullary thyroid carcinoma. *Fam Cancer* **7**: 141–149.

Ribeiro AS, Albergaria A, Sousa B, Correia AL, Bracke M, Seruca R *et al*. (2010). Extracellular cleavage and shedding of P-cadherin: a mechanism underlying the invasive behaviour of breast cancer cells. *Oncogene* **29**: 392–402.

Ribeiro FR, Meireles AM, Rocha AS, Teixeira MR. (2008). Conventional and molecular cytogenetics of human non-medullary thyroid carcinoma: characterization of eight cell line models and review of the literature on clinical samples. *BMC Cancer* **8**: 371.

Rikitake Y, Moran E. (1992). DNA-binding properties of the E1A-associated 300-kilodalton protein. *Mol Cell Biol* **12**: 2826–2836.

Roy R, Yang J, Moses MA. (2009). Matrix metalloproteinases as novel biomarkers and potential therapeutic targets in human cancer. *J Clin Oncol* **27**: 5287–5297.

Schweppe RE, Klopper JP, Korch C, Pugazhenthi U, Benezra M, Knauf JA *et al*. (2008). Deoxyribonucleic acid profiling analysis of 40 human thyroid cancer cell lines reveals cross-contamination resulting in cell line redundancy and misidentification. *J Clin Endocrinol Metab* **93**: 4331–4341.

Shiroshima T, Oka C, Kawaichi M. (2009). Identification of LRP1B-interacting proteins and inhibition of protein kinase Calpha-phosphorylation of LRP1B by association with PICK1. *FEBS Lett* **583**: 43–48.

Song H, Li Y, Lee J, Schwartz AL, Bu G. (2009). Low-density lipoprotein receptor-related protein 1 promotes cancer cell migration and invasion by inducing the expression of matrix metalloproteinases 2 and 9. *Cancer Res* **69**: 879–886.

Stankov K, Pastore A, Toschi L, McKay J, Lesueur F, Kraimps JL *et al*. (2004). Allelic loss on chromosomes 2q21 and 19p 13.2 in oxyphilic thyroid tumors. *Int J Cancer* **111**: 463–467.

Suh I, Filetti S, Vriens MR, Guerrero MA, Tumino S, Wong M *et al*. (2009). Distinct loci on chromosome 1q21 and 6q22 predispose to familial nonmedullary thyroid cancer: a SNP array-based linkage analysis of 38 families. *Surgery* **146**: 1073–1080.

Tanaga K, Bujo H, Zhu Y, Kanaki T, Hirayama S, Takahashi K *et al*. (2004). LRP1B attenuates the migration of smooth muscle cells by reducing membrane localization of urokinase and PDGF receptors. *Arterioscler Thromb Vasc Biol* **24**: 1422–1428.

Toth M, Muller U, Doerfler W. (1990). Establishment of de novo DNA methylation patterns. Transcription factor binding and deoxycytidine methylation at CpG and non-CpG sequences in an integrated adenovirus promoter. *J Mol Biol* **214**: 673–683.

Ulisse S, Baldini E, Sorrenti S, D′Armiento M. (2009). The urokinase plasminogen activator system: a target for anti-cancer therapy. *Curr Cancer Drug Targets* **9**: 32–71.

Walker LC, Harris GC, Wells JE, Robinson BA, Morris CM. (2008). Association of chromosome band 8q22 copy number gain with high grade invasive breast carcinomas by assessment of core needle biopsies. *Genes Chromosomes Cancer* **47**: 405–417.

Woodcock DM, Lawler CB, Linsenmeyer ME, Doherty JP, Warren WD. (1997). Asymmetric methylation in the hypermethylated CpG promoter region of the human L1 retrotransposon. *J Biol Chem* **272**: 7810–7816.

Yang Z, Strickland DK, Bornstein P. (2001). Extracellular matrix metalloproteinase 2 levels are regulated by the low density lipoprotein-related scavenger receptor and thrombospondin 2. *J Biol Chem* **276**: 8403–8408.

Supplementary Information accompanies the paper on the Oncogene website (http://www.nature.com/onc)